CHAPTER - 4

PHYSICAL PROPERTIES OF THREE BICYCLOHEXANE COMPOUNDS POSSESSING SMECTIC B PHASE I : X-RAY DIFFRACTION STUDY

4.1 Introduction

Liquid crystal material research has gained considerable importance due to their increased applicability in display devices. At the same time these compounds exhibit a wide variety of phase transitions study of which play an important role in the development of the modern theory of phase transitions and critical phenomena. Quantitative knowledge of orientational ordering and better understanding of the molecular structure of liquid crystals are required so that improved materials may be produced for applications. Study of pure compounds is also an important prerequisite in the preparation of mixtures better tuned to meet the specific demands of electro-optic display devices. In this chapter, I present the results of x-ray diffraction measurements on three non-polar alkenyl/alkenyloxy bicyclohexane compounds possessing smectic B phase, which is precursor of nematic phase in two of the compounds, while in case of the third compound the smectic B phase is followed directly by isotropic liquid. These compounds are of extraordinary interest since they do not contain any rigid aromatic core, common to most liquid crystalline compounds. They belong to a new class of liquid crystals, recently synthesised, exhibiting low optical anisotropy ($\Delta n < 0.1$), low rotational viscosity, low magnetic anisotropy ($\Delta\chi \approx 0$) and low viscoelastic ratios leading to faster response times in field effect liquid crystal displays [1]. Although some work on bicyclohexane compounds have been reported [1], no x-ray work has been done on these compounds.

In the present chapter x-ray diffraction measurements have been undertaken to investigate the Bond Orientational Order (BOO) in the smectic B phase of all the compounds. As suggested by Birgeneau and Litster [2], the smectic B phase is a

realisation of the stacked hexagonal phase possessing BOO found in two dimensions. In such systems with six fold symmetry the BOO is defined to be the thermal average of the quantity,

$$\Psi(\vec{r})=\langle \exp(i6\theta(\vec{r})\rangle \qquad (4.1)$$

where, $\theta(\vec{r})$ is the angle a nearest neighbour bond at the point $\vec{r}$ makes with a reference direction in the plane. Although x-ray [3] and electron diffraction [4] studies on smectic B phase have been reported, not much work has been done to determine the BOO. The experimentally determined bond orientational order values have been utilised to charecterise the smectic B phase in these compounds which is found to be of the Crystal B type.

Orientational order parameter, intermolecular distance, layer thickness and apparent molecular length throughout the mesomorphic range of all the three compounds have also been reported in this chapter. Translational order parameters (τ) have been measured for one of the compound only, where second order diffraction in the meridional direction have been observed. The experimental order parameters have been fitted to McMillan's theory [5-6] for smectic A phase and the agreement is found to be fairly good.

4.2 Experimental

4.2.1 Materials and texture study

The compounds were donated to us by M/S Hoffmann-La-Roche and Co., Basel, Switzerland. They were used without further purification, since the transition temperatures of the chemicals as seen under a polarising microscope, equipped with a Mettler FP80/82 Thermosystem, agreed with the supplied values

(Hoffmann-La-Roche Catalogue). The structural formula, chemical names and transition temperatures of the compounds are as follows :-

(I) 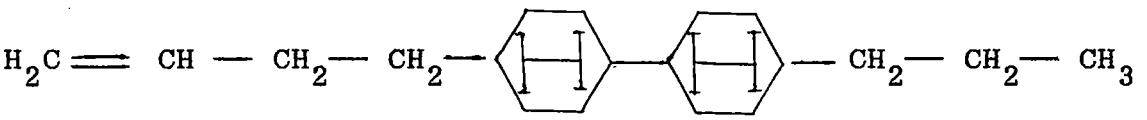

4(3″ - butenyl)4′(propyl) 1,1′ bicyclohexane (BPBCH in short)

C(18°C)Sm B(73°C)N(77°C)I

(II) 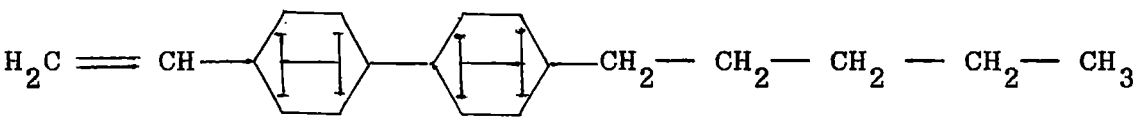

4 - Vinyl, 4′-n-pentyl bicyclohexane (VPBCH in short)

C(-8°C)Sm B(52°C)N(63°C)I

(III) 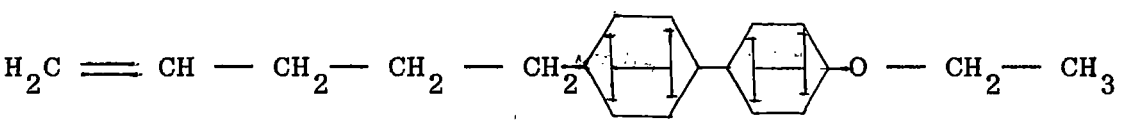

4-ethoxy,4′-Pent-4″-enyl bicyclohexane (EPEBCH in short)

C(11°C)Sm B(43°C)I

The textures of the compounds were observed under a polarising microscope. The observations were performed under crossed polarisers with magnification 150X and samples were taken between a glass slide and a coverslip. Typical marbled textures were observed in the nematic phases of BPBCH and VPBCH. The smectic B phase of BPBCH showed mosaic texture, while VPBCH and EPEBCH showed typical smectic B texture with double refracting lancets and pseudoisotropic regions.

4.2.2 X-ray diffraction study

A detailed description of the experimental set-up for x-ray diffraction has been given by Jha et al [7]. The sample was enclosed in a thin-walled lithium glass capillary of 1mm diameter. The capillary containing the sample was inserted in a thermally insulated brass block, the temperature of which was measured and regulated by a temperature controller (Indotherm model IT401D), within an accuracy of $\pm 0.5^{\circ}C$. X-ray diffraction patterns were recorded photographically on a flat plate camera using Ni filtered Cu K_{α} radiation of wavelength $\lambda=1.5418\text{Å}$. For x-ray diffraction study these compounds could not be aligned even in a magnetic field of about 0.6T. Magnetic susceptibility anisotropy, $\Delta\chi$, for these compounds being almost zero, it is not possible to obtain monodomain samples by application of magnetic field. However, aligned specimens in which the hexagonal symmetry of the smectic B phase extended throughout the bulk samples could be prepared for all these compounds by controlled cooling (0.1deg/min), of the samples kept in 1 mm diameter glass capillaries, from the isotropic state to room temperature ($\sim 20^{\circ}C$). By trial one of the monodomain samples was selected in which the capillary could be rotated in such a manner that the director (or the layer normal) coincided with the direction of the x-ray beam. At this position of the capillary x-ray diffraction photographs were recorded at regular temperature intervals from $\sim 20^{\circ}C$ upto the isotropic state. Due to lack of thermostatic arrangement with cooling facilities in our laboratory, photographs below room temperature could not be taken. Photographs for orientational order parameter measurements were taken after rotating the sample filled capillary 90 degrees with respect to the previous position such that the direction of the x-ray beam was parallel to the smectic

layer. To obtain better accuracy in the measurement of layer spacing, the film was kept at a distance of about 9cm from the samples. This procedure was followed for each compound.

The x-ray photographs were scanned both linearly and circularly by an optical densitometer (VEB Carl Zeiss Jena Model 100). Measured optical densities were converted to x-ray intensities with the help of a calibration curve following the procedure of Klug and Alexander [8] as described in detail in chapter 2.

4.3 Results and Discussions

4.3.1 Bond orientational order

Figures 4.1(a)-4.1(c) shows the x-ray diffraction photographs of the aligned sample in the smectic B phase of BPBCH, VPBCH and EPEBCH at 59°C, 30°C and 20°C respectively, with the incident x-ray beam parallel to the layer normal. The outer diffraction ring is split up into six spots, clearly showing the hexagonal molecular arrangement within the layers of the phase. Almost identical photographs have been obtained from room temperature ($\sim$ 20°C) upto the smectic B to nematic (or isotropic) transition temperature in all the three compounds under study.

The Bond Orientational Order (BOO) can be written as

$$\langle\cos(6\theta)\rangle = \int_0^{\pi/6}\cos(6\theta)f(\theta)d\theta \Big/ \int_0^{\pi/6} f(\theta)d\theta \qquad (4.2)$$

where $f(\theta)$ is the angular distribution function of centre of mass of the neighbouring molecules with respect to a central molecule and the angular distribution function has a maximum at θ = 0. However, the BOO can be approximated by the following

Figure 4.1(a) X-ray diffraction photograph of aligned sample of BPBCH recorded at 59°C (smectic B phase).

Figure 4.1(b) X-ray diffraction photograph of aligned sample of VPBCH recorded at 30°C (smectic B phase).

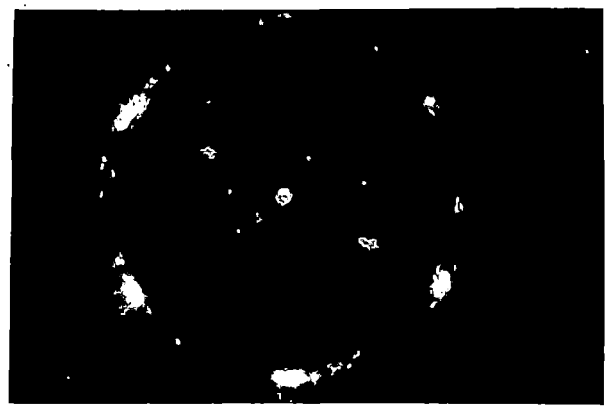

Figure 4.1(c) X-ray diffraction photograph of aligned sample of EPEBCH recorded at 20°C (smectic B phase).

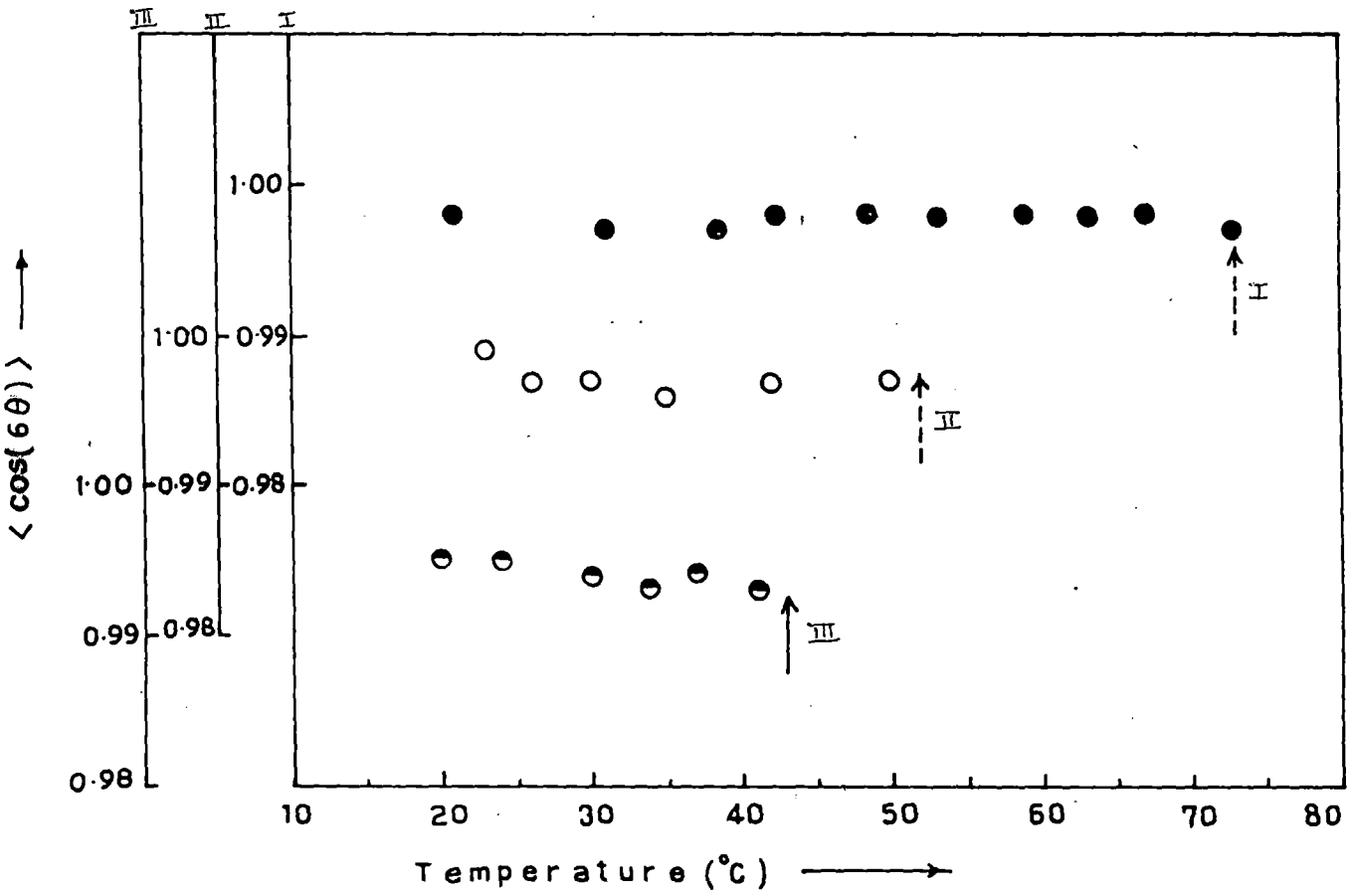

Figure 4.2 Temperature variation of bond orientatational of the three compounds. •, BOO value for BPBCH; o, BOO vaue for VPBCH; ⊖, BOO value for EPEBCH. ↑ indicates smectic B - nematic transition temperature, ↑ indicates smectic B - isotropic transition temperature.

expression, i.e.,

$$\langle\cos(6\theta)\rangle \approx \int_0^{\pi/6}\cos(6\theta)I(\theta)d\theta \Big/ \int_0^{\pi/6}I(\theta)d\theta \qquad (4.3)$$

where $I(\theta)$ is the azimuthal distribution of the x-ray diffraction intensity. Following Vainshtein [9] it has been assumed that $I(\theta)$, the intensity distribution, is proportional to $f(\theta)$ the distribution function and consequently has its maximum at $\theta = 0$ also. The experimental x-ray intensity profile for each peak has been corrected for broadening due to the width of the primary x-ray beam, using a method of deconvolution based on substitution of successive foldings [10], as described in chapter 2.

Table 4.1 shows the bond orientational order values at different temperatures in the smectic B phase of BPBCH, VPBCH and EPEBCH. The BOO's for all the three compounds are found to be almost equal to unity and independent of temperature throughout the smectic B phase (Figures 4.2(a)-4.2(c)). This result seems to indicate that the smectic B modification in these compounds are in fact of the Crystal B type in the sense that the molecular positions exhibit long range bond orientational order throughout the phase [3].

I have tried to determine the correlation length in the smectic layer plane from linear scan of the diffraction peaks. X-ray intensities were at first corrected for the use of a flat film. This corrected intensity data was then deconvoluted for finite width of the collimator. The deconvoluted intensity profile I(q) was fitted to a lorentzian form with a quadratic background, viz.

$$I(q)= \frac{a_1}{a_2+(q - q_o)^2} + a_3q^2 + a_4q + a_5, \qquad (4.4)$$

q being the magnitude of the scattering vector. The correlation length is defined as $\xi = 2\pi(a_2)^{-1/2}$. The values of the correlation lengths obtained in this way varied from 200Å to 270Å for the three compounds. However, for Crystal B phase the correlation lengths are expected to be much longer. One reason for this discrepancy may be due to the use of Ni filtered Cu K_α radiation, which contains a white background in addition to the Cu K_α peak. No correction for this white radiation, which broadens the diffraction peaks considerably, is made here. Hence, the experimental values of correlation lengths as obtained above are much shorter than the theoretically expected values.

4.3.2 Orientational order parameter and molecular parameters

The angular distribution of the x-ray diffraction intensities were utilised to obtain the orientational distribution function $f(\theta)$ [11] and hence the orientational order parameters (OOP) $\langle P_2 \rangle$ and $\langle P_4 \rangle$ following a procedure reported earlier [12]. The mean intensity values of the four quadrants are given in tables 4.2-4.4 for the three compounds. Tables 4.5-4.7 include the normalised distribution function $f(\beta)$ values for different temperatures at 5° intervals, calculated from the equation 2.15 described in chapter 2. The procedure for calculating $\langle P_2 \rangle$ and $\langle P_4 \rangle$ values has also been described in chapter 2. The values of $\langle P_2 \rangle$ and $\langle P_4 \rangle$ at different temperatures for the three compounds are arranged in tables 4.8-4.10. Figures 4.3(a)-4.3(c) show the variation of the experimentally determined OOP's with temperature for all the samples studied. The experimental $\langle P_2 \rangle$

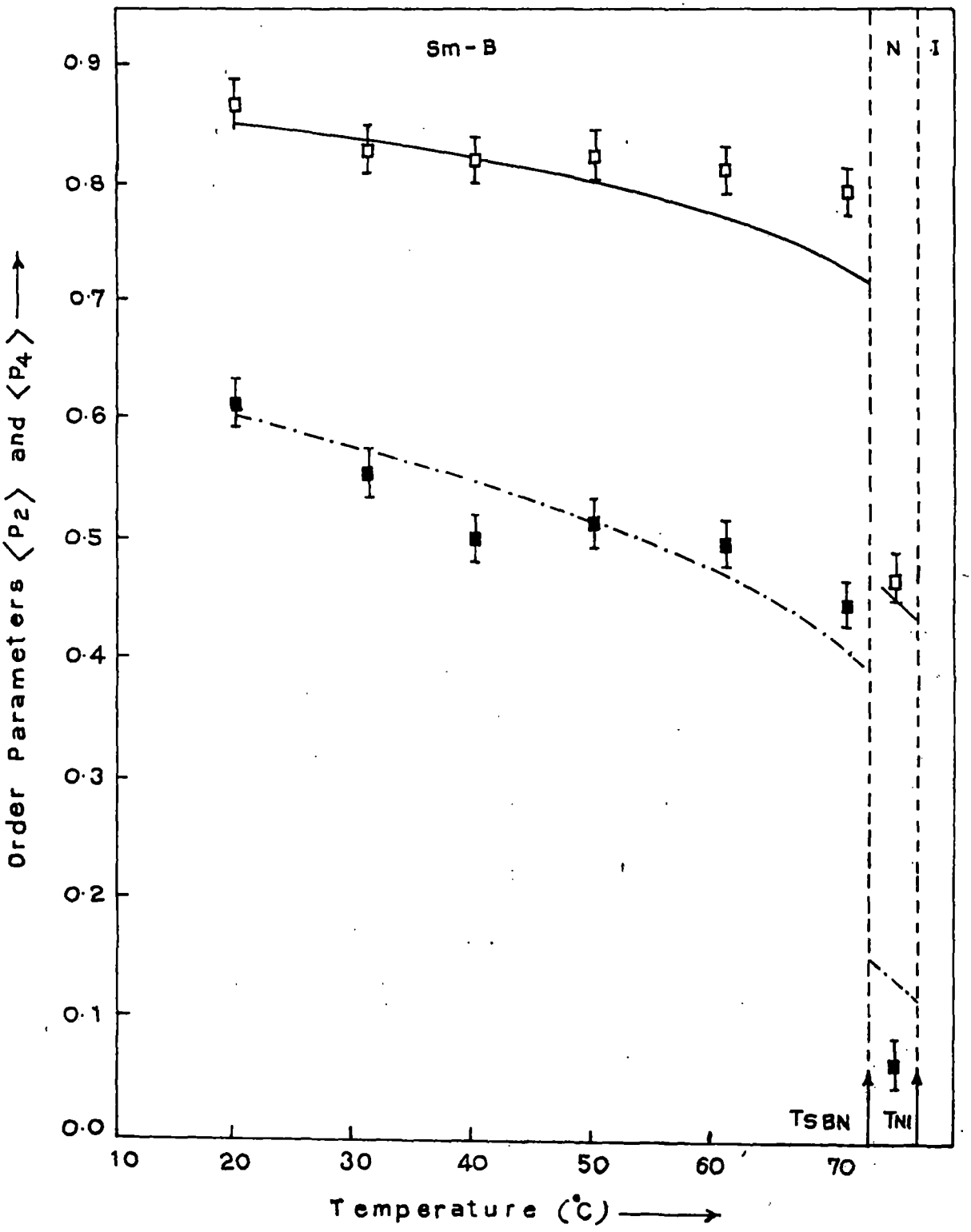

Figure 4.3(a) Temperature variation of $\langle P_2 \rangle$ and $\langle P_4 \rangle$ for BPBCH. □, $\langle P_2 \rangle$ from x-ray data; ■, $\langle P_4 \rangle$ from x-ray data; full line McMillan $\langle P_2 \rangle$ value; dashed line McMillan $\langle P_4 \rangle$ value; $\alpha=0.96$ and $\delta=0$, values of McMillan potential parameters. T_{SBN}= smectic B-nematic tansition temperature T_{NI}=nematic-isotropic transition temperature. Vertical bars show estimated errors.

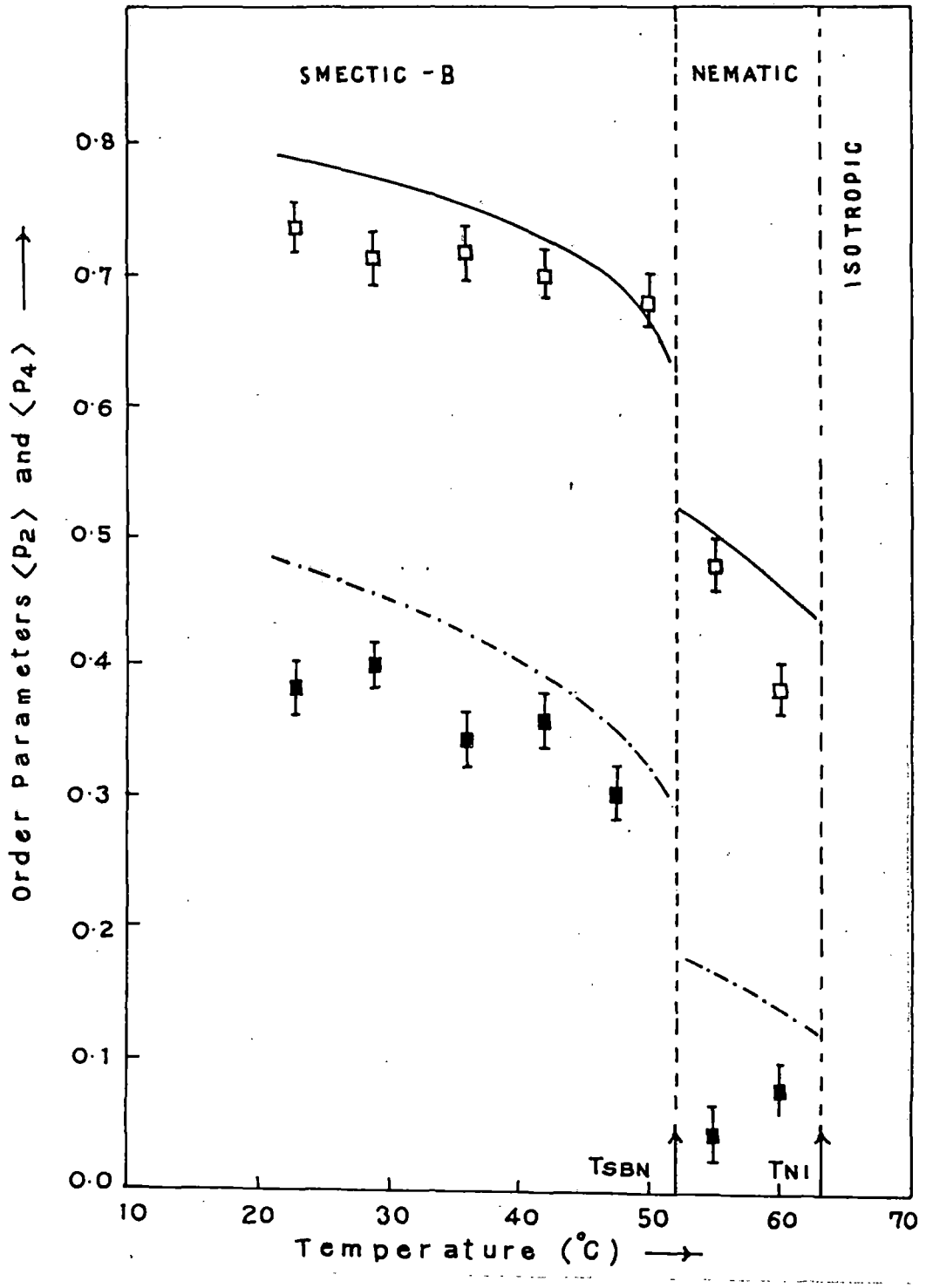

Figure 4.3(b) Temperature variation of $\langle P_2 \rangle$ and $\langle P_4 \rangle$ for VPBCH. □, $\langle P_2 \rangle$ from x-ray data; ■, $\langle P_4 \rangle$ from x-ray data; full line McMillan $\langle P_2 \rangle$ value; dashed line McMillan $\langle P_4 \rangle$ value; α=0.65 and δ=0.245, values of McMillan potential parameters. $T_{SB\ N}$= smecticB - nematic tansition temperature $T_{N\ I}$= nemati c-isotropic transition temperature. Vertical bars show estimated errors.

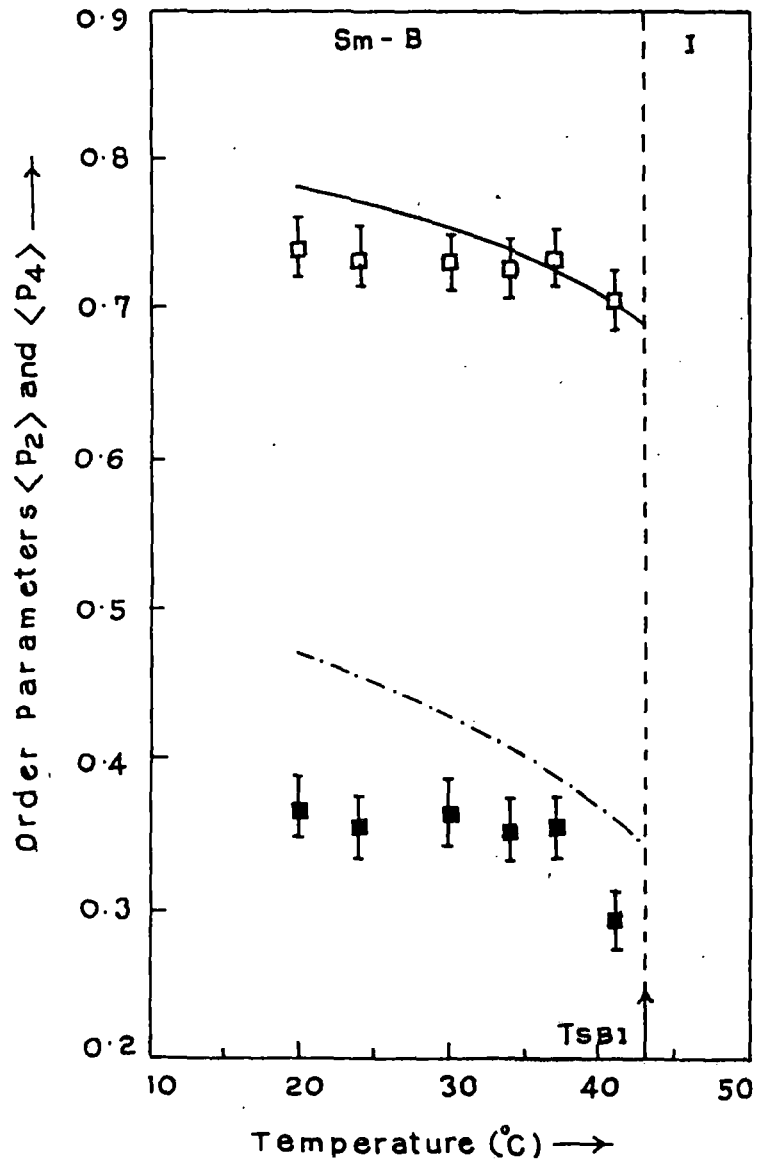

Figure 4.3(c) Temperature variation of $\langle P_2 \rangle$ and $\langle P_4 \rangle$ for EBEBCH. □, $\langle P_2 \rangle$ from x-ray data; ■, $\langle P_4 \rangle$ from x-ray data; full line McMillan $\langle P_2 \rangle$ value; dashed line McMillan $\langle P_4 \rangle$ value; α=0.714 and δ=0.251, values of McMillan potential parameters. T_{SBI}= smectic B-isotropic transition temperature. Vertical bars show estimated errors.

and $\langle P_4 \rangle$ values are found to vary very little with temperature within the smectic B phase. OOP values in the nematic phase of BPBCH and VPBCH however show marked temperature dependence. These values are also relatively high in the smectic B phase, showing the phase to be much more orientationally ordered than the neighbouring nematic phase. The smectic B to nematic phase transitions in BPBCH and VPBCH are clearly of the first order as can be seen from the abrupt jump in the order parameter values of these two compounds near the transition temperature. This again indicates that the smectic B phases of these compounds are the crystal B phases, unlike the hexatic B phase which undergoes a second order phase transition [13]. It may be mentioned that although the approximation used for calculating $\langle P_L \rangle$ (L= 2,4) is not valid for $\langle P_2 \rangle \gtrsim 0.8$ [11] (as in the case of BPBCH) I am still reporting these OOP values since at least qualitatively they show the degree of order of a liquid crystal in smectic B phase for which such values are rare.

I tried to fit the experimental order parameter values for these compounds to those calculated from McMillan's theory [5,6] for smectic A phase, using the potential parameters δ and α as adjustable constants, for the lack of other alternatives. The best fit theoretical curves are given in the respective figures (Figures 4.3(a)-4.3(c)) and the values of δ and α used for the calculations are given in the corresponding figure captions. The agreement seems to be fairly good for BPBCH and fair for other two compounds even though this theory is not strictly applicable to the smectic B phase.

I have also determined the translational order parameter τ for VPBCH (where second order reflections are present) from the experimental data using a simple procedure described by Leadbetter and Norris [11]. According to McMillan [6], the smectic layer distribution functions are directly related to the

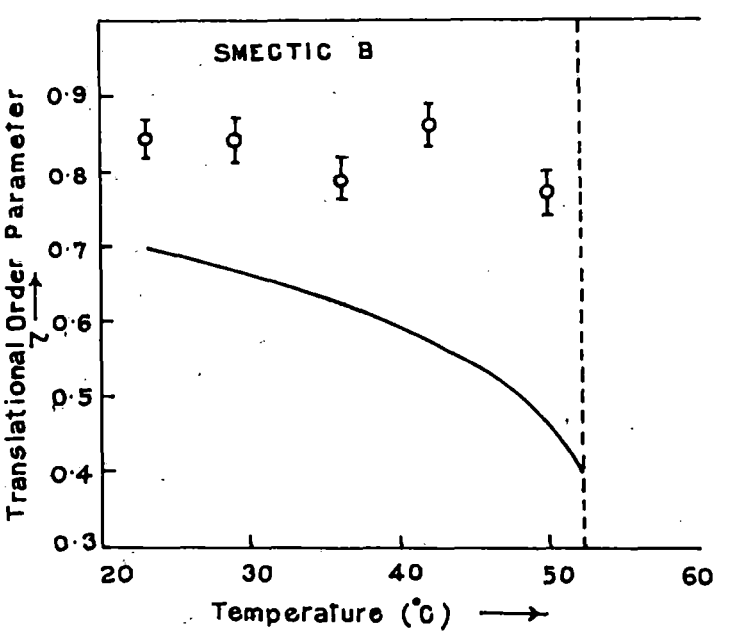

Figure 4.4 The translational order parameter τ for the smectic phase of VPBCH. o, Experimental; ———, theoretical values. Vertical bars show estimated errors.

intensity of the layer reflection. Hence the intensity of (00m) layer reflection can be expressed as

$$I(00m) = C\tau_m^2 \langle F(00m) \rangle^2 \qquad (4.5)$$

where C is a constant and F(00m) is the structure factor for a smectic layer and τ_1 is the translational order parameter. For gaussian distribution of the translational distribution function Leadbetter et al [14] derived the following relation

$$\tau_m = \tau_1^{m^2} \qquad (4.6)$$

I have measured I(002)and I(001) for VPBCH at different temperatures in the smectic B phase. The intensity values are corrected for use of flat plate camera and then assuming F(001)

$$\approx \frac{I(002)}{I(001)} = \tau_2^2 / \tau_1^2 = \tau_1^6 \qquad (4.7)$$

Using equation (4.7), the translational order parameters τ (= τ_1) have been calculated and these are compared with the values obtained from McMillan's theory as shown in figure 4.4. These τ values are much larger than those calculated from McMillan's theory. This deviation may be partly due to the assumption of gaussian distribution of molecules normal to the smectic layer in calculating τ [15]. and partly due to the fact that McMillan's theory is not applicable to smectic B phase. However it is gratifying to note that the experimental τ values are significantly larger than those calculated for smectic A phase, which is in accord with the fact that smectic B phase is more ordered phase than smectic A phase. Table 4.11 include the values of τ_1 at different temperatures in the smectic B phase of VPBCH.

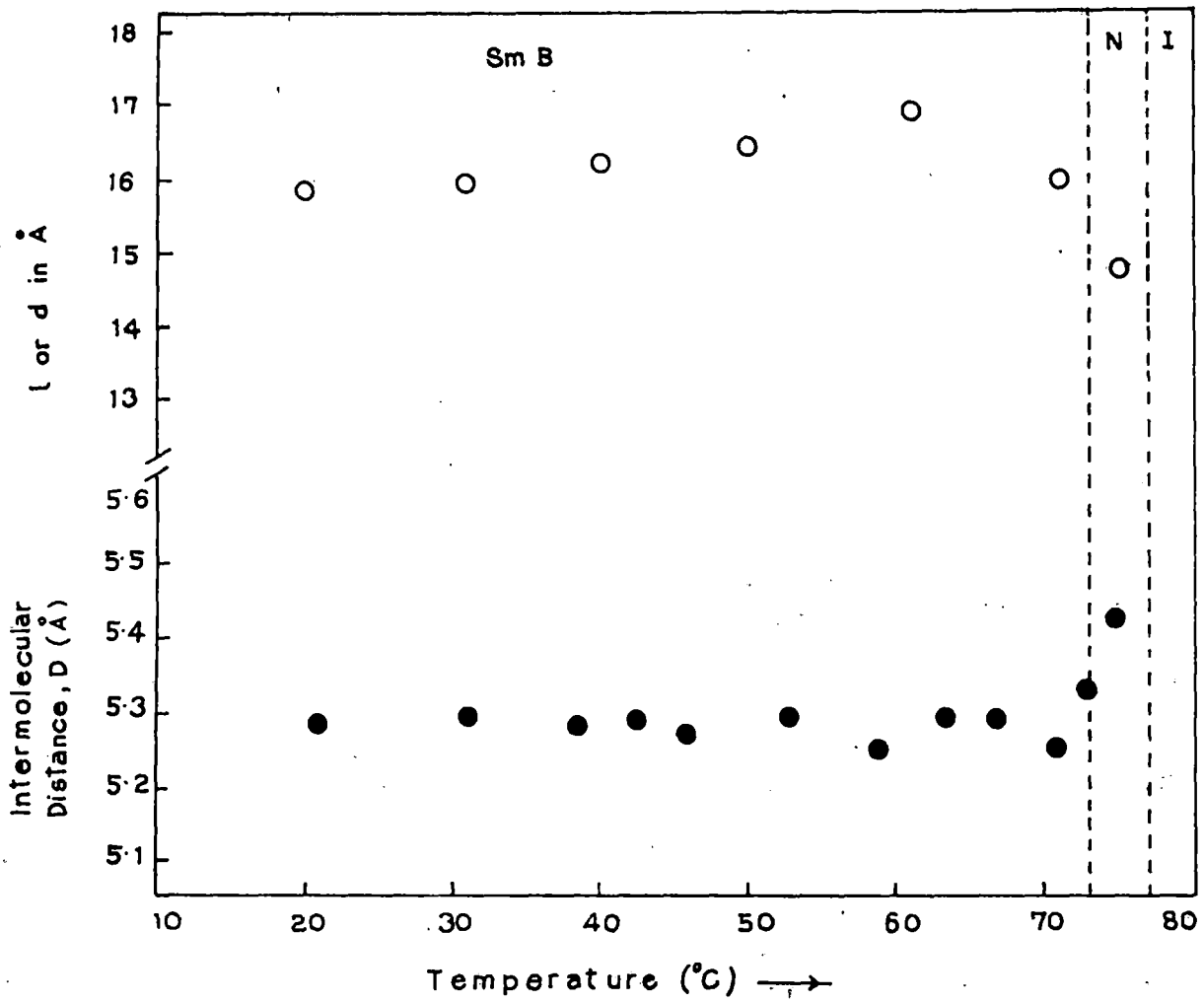

Figure 4.5(a) Variation of layer thickness,d, or apparent molecular length, l, and intermolecular distance, D with temperature for BPBCH. o, d or l value; ●, D value. Estimated errors are smaller than the size of the symbols used.

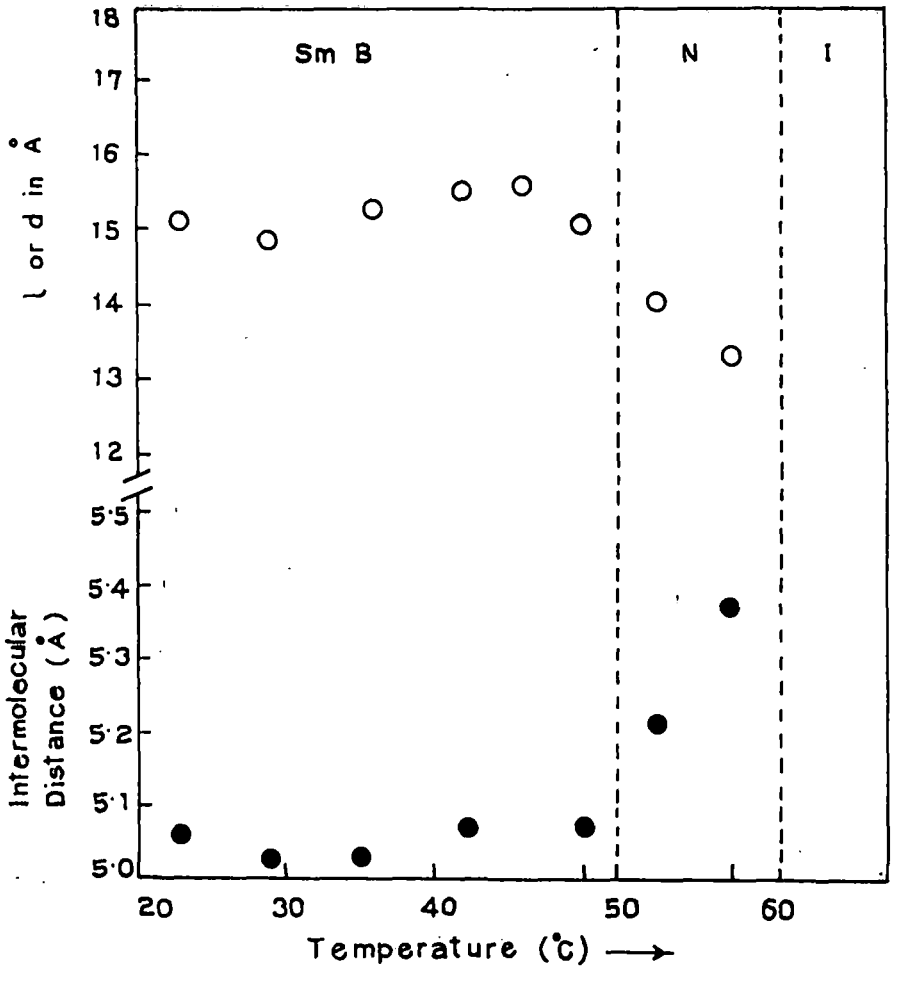

Figure 4.5(b) Variation of layer thickness,d, or apparent molecular length, l, and intermolecular distance, D with temperature for VPBCH. o, d or l value; ●, D value. Estimated errors are smaller than the size of the symbols used.

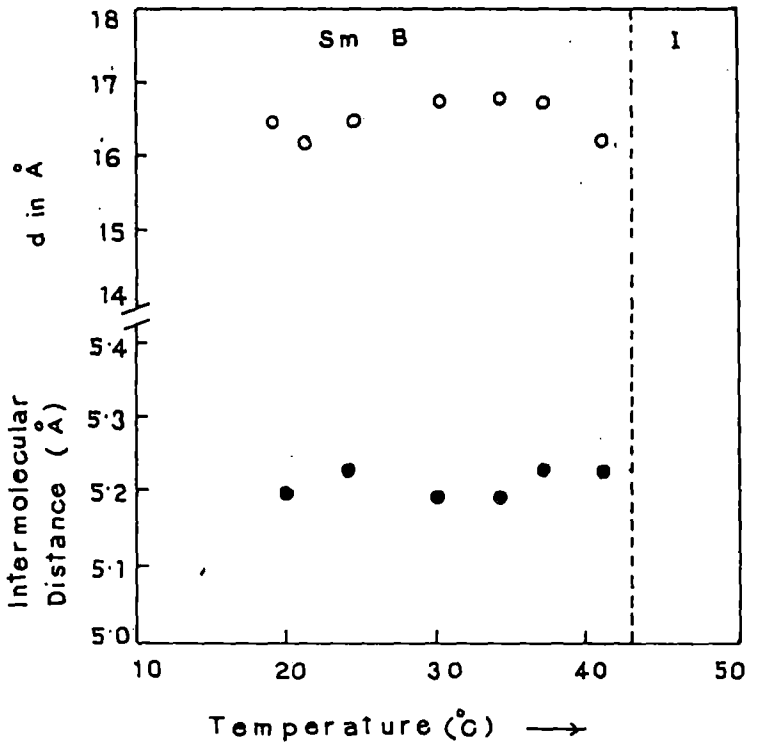

Figure 4.5(c) Variation of layer thickness, d, and intermolecular distance, D with temperature for EPEBCH. o: d value; ●: D value. Estimated errors are smaller than the size of the symbols used.

The values of the apparent molecular length (l) or layer thickness (d) and the intermolecular distance, D, at different temperatures for BPBCH, VPBCH and EPEBCH are given in tables 4.12 and 4.13 respectively. The temperature variations of d in the smectic phase and l in the nematic phase (where it is present) for the three compounds are shown in Figures 4.5(a)-4.5(c). Also shown on the same figures are the temperature dependences of the intermolecular distance, D, for these compounds. As expected the temperature variations of d and l are slight. However, for all the compounds, the layer thickness at first increases with increasing temperature but then decreases just before smectic to nematic (or isotropic) phase transition. This decrease before the phase transition is not difficult to understand, since the effective lengths of the molecules decrease due to increasing thermal vibrations of its chain part just before the transition. The low temperature variation in the layer thickness may be due to the geometry of packing in the smectic layer at these temperatures. In all the compounds the layer thicknesses are almost equal to the respective model molecular lengths (15.6 Å for BPBCH 15.25 Å for VPBCH and 16.5 Å for EPEBCH molecule) The apparent molecular lengths in nematic phase of BPBCH and VPBCH are significantly smaller than the layer thicknesses in the corresponding smectic B phases. This is not surprising considering the flexible nature of the molecules. The lateral distances of the molecules, D, in the nematic phase are significantly larger than the values observed in the case of nematics with rigid core ($\lesssim$ 5Å). Also, the temperature variations of D in the nematic phase are quite rapid, caused once again by the thermal vibrations of these flexible molecules.

Table 4.1

Bond orientational order ($\langle\cos(6\theta)\rangle$) values at different temperatures in the the smectic B phase of BPBCH, VPBCH and EPEBCH.

BPBCH		VPBCH		EPEBCH	
Temp/^{o}C	$\langle\cos(6\theta)\rangle$	Temp/^{o}C	$\langle\cos(6\theta)\rangle$	Temp/^{o}C	$\langle\cos(6\theta)\rangle$
21.0	0.998	23.0	0.999	20.0	0.995
31.0	0.997	26.0	0.997	24.0	0.995
38.5	0.997	30.0	0.997	30.0	0.994
42.5	0.998	35.0	0.996	34.0	0.993
48.5	0.998	42.0	0.997	37.0	0.994
53.0	0.998	50.0	0.997	41.0	0.993
59.0	0.998				
63.5	0.998				
67.0	0.998				
73.0	0.997				

Table 4.2

Experimental intensity values I(ψ), in arbitrary units, of BPBCH after background correction.

ψ (degree)	I(ψ) values at different temperatures in ^{o}C						
	20.0	31.0	40.0	50.0	61.0	71.0	75.0
0	9.3	11.5	11.4	9.5	7.3	6.2	9.3
5	8.7	11.2	11.3	9.1	7.1	6.0	9.1
10	7.4	10.4	10.5	8.4	6.3	5.4	8.7
15	5.7	8.9	8.8	6.8	4.9	4.5	8.1
20	3.9	6.1	6.1	4.7	3.3	3.4	7.5
25	1.9	3.0	3.8	2.6	1.7	2.4	6.7
30	0.0	1.4	1.8	1.2	1.2	1.5	5.8
35	0.0	0.5	0.6	0.6	0.7	0.6	5.0
40	0.0	0.0	0.1	0.2	0.4	0.2	4.1
45	0.0	0.0	0.0	0.0	0.0	0.0	3.5
50	0.0	0.0	0.0	0.0	0.0	0.0	2.8
55	0.0	0.0	0.0	0.0	0.0	0.0	2.0
60	0.0	0.0	0.0	0.0	0.0	0.0	1.5
65	0.0	0.0	0.0	0.0	0.0	0.0	1.0
70	0.0	0.0	0.0	0.0	0.0	0.0	0.7
75	0.0	0.0	0.0	0.0	0.0	0.0	0.4
80	0.0	0.0	0.0	0.0	0.0	0.0	0.2
85	0.0	0.0	0.0	0.0	0.0	0.0	0.2
90	0.0	0.0	0.0	0.0	0.0	0.0	0.0

Table 4.3

Experimental intensity values I(ψ), in arbitrary units, of VPBCH after background correction.

ψ (degree)	I(ψ) values at different temperatures in ^{o}C						
	23.0	29.0	36.0	42.0	50.0	55.0	60.0
0	15.1	16.9	10.0	17.6	10.3	1.4	1.2
5	15.1	16.9	9.3	17.3	10.1	1.5	1.2
10	14.0	16.2	7.9	16.7	9.4	1.5	1.1
15	10.7	14.4	5.9	14.8	8.0	1.3	1.0
20	8.0	8.6	4.5	11.6	6.3	1.2	0.9
25	5.4	5.2	3.0	7.2	4.5	1.0	0.8
30	3.7	3.3	1.8	4.4	3.2	0.9	0.7
35	2.5	2.3	1.2	2.9	2.3	0.8	0.6
40	1.5	1.7	0.8	1.8	1.7	0.7	0.5
45	0.9	1.2	0.5	1.3	1.2	0.6	0.5
50	0.7	1.0	0.4	1.0	0.8	0.5	0.4
55	0.5	0.8	0.2	0.8	0.5	0.4	0.4
60	0.3	0.6	0.1	0.6	0.3	0.3	0.3
65	0.1	0.5	0.0	0.5	0.2	0.1	0.3
70	0.0	0.4	0.0	0.4	0.1	0.0	0.2
75	0.0	0.3	0.0	0.3	0.0	0.0	0.2
80	0.0	0.2	0.0	0.2	0.0	0.0	0.2
85	0.0	0.1	0.0	0.2	0.0	0.0	0.1
90	0.0	0.0	0.0	0.1	0.0	0.0	0.1

Table 4.4

Experimental intensity values $I(\psi)$, in arbitrary units, of EPEBCH after background correction.

ψ (degree)	$I(\psi)$ values at different temperatures in ^{o}C					
	20.0	24.0	30.0	34.0	37.0	41.0
0	14.3	8.6	7.8	8.4	7.4	6.4
5	14.3	8.4	7.7	8.1	7.3	6.3
10	13.4	7.8	7.0	7.7	6.8	5.8
15	10.8	6.7	5.8	6.8	5.8	5.0
20	7.8	5.2	4.6	5.4	4.5	4.1
25	5.7	3.5	2.9	3.6	3.3	3.2
30	3.7	2.3	2.0	2.2	2.1	2.4
35	2.5	1.6	1.3	1.4	1.3	1.6
40	1.7	1.0	0.9	0.9	0.8	1.0
45	1.1	0.6	0.6	0.6	0.5	0.6
50	0.6	0.3	0.4	0.4	0.3	0.3
55	0.2	0.2	0.2	0.2	0.2	0.0
60	0.0	0.1	0.1	0.2	0.1	0.0
65	0.0	0.0	0.1	0.1	0.0	0.0
70	0.0	0.0	0.0	0.1	0.0	0.0
75	0.0	0.0	0.0	0.0	0.0	0.0
80	0.0	0.0	0.0	0.0	0.0	0.0
85	0.0	0.0	0.0	0.0	0.0	0.0
90	0.0	0.0	0.0	0.0	0.0	0.0

Table 4.5

Normalised distribution function $f(\beta)$ values of BPBCH at different temperatures.

β (degree)	$f(\beta)$ values at different temperatures in ^{o}C						
	20.0	31.0	40.0	50.0	61.0	71.0	75.0
0	15.62	11.11	11.51	12.02	13.66	10.87	4.08
5	15.11	11.15	11.24	11.82	13.10	10.53	4.01
10	13.52	10.93	10.33	11.08	11.50	9.56	3.82
15	10.86	9.83	8.64	9.50	9.10	8.11	3.54
20	7.46	7.59	6.30	7.10	6.36	6.37	3.19
25	4.07	4.70	3.80	4.39	3.84	4.56	2.82
30	1.47	2.11	1.75	2.10	1.98	2.86	2.42
35	0.07	0.51	0.52	0.69	0.92	1.47	2.04
40	-0.29	-0.05	0.06	0.15	0.46	0.53	1.67
45	-0.13	-0.01	0.02	0.09	0.28	0.05	1.35
50	0.06	0.01	0.05	0.11	0.15	-0.08	1.06
55	0.09	0.07	0.02	0.05	0.01	-0.03	0.81
60	0.02	-0.03	-0.03	-0.03	-0.08	0.03	0.59
65	-0.04	-0.07	-0.04	-0.06	-0.07	0.04	0.40
70	-0.03	-0.03	0.00	-0.02	-0.01	0.01	0.24
75	0.00	0.03	0.03	0.03	0.04	-0.02	0.13
80	0.02	0.03	0.03	0.03	0.03	-0.02	0.06
85	0.00	0.00	0.00	0.00	0.00	0.00	0.03
90	0.00	-0.02	-0.02	-0.02	-0.02	0.01	0.02

Table 4.6

Normalised distribution function $f(\beta)$ values of VPBCH at different temperatures.

β (degree)	$f(\beta)$ values at different temperatures in ^{o}C						
	20.0	29.0	36.0	42.0	50.0	55.0	60.0
0	10.74	9.03	8.91	7.33	8.27	3.77	4.21
5	10.36	9.14	8.73	7.51	8.13	3.83	4.11
10	9.28	9.12	8.13	7.76	7.64	3.91	3.84
15	7.62	8.29	7.08	7.45	6.69	3.81	3.42
20	5.66	6.39	5.64	6.22	5.31	3.39	2.93
25	3.77	3.93	4.04	4.33	3.77	2.76	2.43
30	2.30	1.81	2.60	2.44	2.42	2.15	1.99
35	1.29	0.65	1.53	1.15	1.50	1.74	1.63
40	0.77	0.40	0.88	0.56	0.99	1.57	1.35
45	0.52	0.51	0.53	0.42	0.73	1.50	1.14
50	0.36	0.52	0.35	0.37	0.54	1.36	0.97
55	0.23	0.33	0.23	0.27	0.34	1.09	0.82
60	0.11	0.11	0.13	0.15	0.18	0.72	0.69
65	0.04	0.03	0.05	0.08	0.08	0.37	0.57
70	0.02	0.09	0.02	0.08	0.04	0.12	0.46
75	0.01	0.14	0.00	0.09	0.03	0.00	0.36
80	0.01	0.11	0.00	0.07	0.02	0.00	0.27
85	0.00	0.02	0.00	0.03	0.00	0.00	0.21
90	0.00	0.00	0.00	0.01	0.00	0.00	0.19

Table 4.7

Normalised distribution function $f(\beta)$ values of EPEBCH at different temperatures.

β (degree)	$f(\beta)$ values at different temperatures in ^{o}C					
	20.0	24.0	30.0	34.0	37.0	41.0
0	9.82	9.06	9.56	7.91	8.65	8.25
5	9.59	8.91	9.36	7.96	8.55	8.00
10	8.86	8.39	8.69	7.90	8.16	7.31
15	7.54	7.34	7.47	7.35	7.29	6.29
20	5.76	5.80	5.79	6.09	5.90	5.12
25	3.89	4.06	3.96	4.35	4.23	3.96
30	2.35	2.54	2.40	2.64	2.66	2.91
35	1.38	1.48	1.36	1.39	1.50	2.02
40	0.89	0.90	0.81	0.73	0.83	1.31
45	0.64	0.59	0.56	0.46	0.50	0.76
50	0.42	0.37	0.39	0.33	0.32	0.37
55	0.18	0.17	0.23	0.21	0.19	0.13
60	0.01	0.03	0.08	0.10	0.08	0.01
65	-0.05	-0.03	0.01	0.03	0.01	-0.02
70	-0.02	-0.01	0.00	0.02	-0.01	-0.01
75	0.02	0.02	0.01	0.02	0.00	0.01
80	0.02	0.02	0.01	0.02	0.00	0.01
85	0.00	0.00	0.00	0.00	0.00	0.00
90	0.00	0.00	0.00	0.00	0.00	0.00

Table 4.8

Sample : BPBCH

Variation of $\langle P_2 \rangle$ and $\langle P_4 \rangle$ with temperature.

Temp. in ^{o}C	$\langle P_2 \rangle$	$\langle P_4 \rangle$
20.0	0.868	0.612
31.0	0.833	0.529
40.0	0.820	0.500
50.0	0.824	0.514
61.0	0.812	0.497
71.0	0.796	0.446
75.0	0.469	0.061

Table 4.9

Sample : VPBCH

Variation of $\langle P_2 \rangle$ and $\langle P_4 \rangle$ with temperature.

Temp. in ^{o}C	$\langle P_2 \rangle$	$\langle P_4 \rangle$
23.0	0.734	0.380
29.0	0.712	0.399
36.0	0.717	0.342
42.0	0.699	0.356
50.0	0.680	0.301
55.0	0.477	0.045
60.0	0.381	0.081

Table 4.10

Sample : EBEBCH

Variation of $\langle P_2 \rangle$ and $\langle P_4 \rangle$ with temperature.

Temp. in ^{o}C	$\langle P_2 \rangle$	$\langle P_4 \rangle$
20.0	0.738	0.367
24.0	0.733	0.356
30.0	0.730	0.364
34.0	0.725	0.354
37.0	0.733	0.355
41.0	0.705	0.294

Table 4.11

Translational order parameter (τ_1) at different temperatures in the smectic B phase of VPBCH.

Temp. in ^{o}C	τ_1
23.0	0.841
29.0	0.840
36.0	0.790
42.0	0.860
50.0	0.767

Table 4.12

Apparent molecular length (l) or layer spacing (d) at different temperatures of BPBCH, VPBCH AND EPEBCH.

BPBCH		VPBCH		EPEBCH	
Temp. in ^{o}C	l or d in $\mathring{A}$	Temp. in ^{o}C	l or d in $\mathring{A}$	Temp. in ^{o}C	l or d in $\mathring{A}$
20.0	15.88	23.0	15.14	19.0	16.48
31.0	15.99	29.0	14.93	21.0	16.19
40.0	16.21	36.0	15.37	24.0	16.48
50.0	16.44	42.0	15.64	30.0	16.75
61.0	16.92	46.0	15.72	34.0	16.75
71.0	15.99	50.0	15.14	37.0	16.61
75.0	14.77	55.0	14.14	41.0	16.22
		60.0	13.44		

Table 4.13

Intermolecular distance (D) at different temperatures of BPBCH, VPBCH AND EPEBCH.

BPBCH		VPBCH		EPEBCH	
Temp. in ^{o}C	D in $\mathring{A}$	Temp. in ^{o}C	D in $\mathring{A}$	Temp. in ^{o}C	D in $\mathring{A}$
21.0	5.29	23.0	5.06	20.0	5.19
31.0	5.30	29.0	5.03	24.0	5.22
38.5	5.29	35.0	5.03	30.0	5.19
42.5	5.30	42.0	5.07	34.0	5.19
48.5	5.28	50.0	5.07	37.0	5.22
53.0	5.30	55.0	5.22	41.0	5.22
59.0	5.26	60.0	5.38		
63.5	5.30				
67.0	5.30				
71.0	5.26				
73.0	5.34				
75.0	5.44				

REFERENCES

[1]. M. Schadt, R. Buchecker and K. Müller, Liq. Cryst.,5, 293 (1989).

[2]. R.J. Birgeneau and J.D. Litster, J.Phys. Letts. 39, L399, (1978).

[3]. C.C. Huang (1992), K.J. Strandburg (Ed.)Bond Orientational Order in Condensed Matter Systems, Springer - Verlag, Berlin - New York, pp. 78-136

[4]. M. Cheng, J.H. Ho, S.W. Hui and R. Pindak, Phys. Rev. Letts. 59, 1112, (1987).

[5]. W.L. McMillan, Phys. Rev., 13, 137, (1971).

[6]. W.L. McMillan, Phys. Rev., A6, 936, (1972).

[7]. B. Jha and R. Paul, Proc. Nucl. Phys. Solid State Phys.Symp., (India), 19C, 491, (1976).

[8]. H.P. Klug and L.E. Alexander,X-ray diffraction procedure for Polycrystalline and Amorphous Materials, John Wiley and Sons, New York, pp. 114-116 and pp. 473-474, (1974).

[9]. B.K. Vainshtein, X-ray diffraction by chain molecules, Elsevier Publishing Co., London, pp. 353-355 (1966).

[10]. S. Ergun, J. Appl. Cryst., 1, 19 (1968).

[11]. A.J. Leadbetter, and E.K. Norris, Mol. Phys., 38, 669, (1979).

[12]. B Bhattacharjee, S. Paul and R. Paul,Mol. Phys.,44, 1391, (1981).

[13]. R. Pindak, D.E. Moncton, S.C. Davey and J.W. Goodby, Phys. Rev. Lett., 46, 1135 (1981).

[14]. A.J. Leadbetter, R.M. Richardson, and C.N. Colling, J. Phys. (Paris), 36, C1-37 (1975).

[15]. A.J. Leadbetter and P.G. Wrighton,J. Phys. (Paris), 40, C3-234, (1979).